metals

MDPI

Article

Effects of *Phyllanthus muellerianus* Leaf-Extract on Steel-Reinforcement Corrosion in 3.5% NaCl-Immersed Concrete

Joshua Olusegun Okeniyi [1,*], Cleophas Akintoye Loto [1,2] and Abimbola Patricia Idowu Popoola [2]

[1] Mechanical Engineering Department, Covenant University, Ota 112001, Nigeria; cleophas.loto@covenantuniversity.edu.ng

[2] Chemical, Metallurgical and Materials Engineering Department, Tshwane University of Technology, Pretoria 0001, South Africa; popoolaAPI@tut.ac.za

* Correspondence: joshua.okeniyi@covenantuniversity.edu.ng; Tel.: +234-806-983-6502

Academic Editors: João Manuel R. S. Tavares and Victor Hugo C. de Albuquerque
Received: 22 May 2016; Accepted: 6 September 2016; Published: 27 October 2016

Abstract: This paper investigates *Phyllanthus muellerianus* leaf-extract effects on steel-reinforcement corrosion in concrete immersed in 3.5% NaCl, simulating saline/marine environment. Different concentrations of the leaf-extract were admixed in steel-reinforced concrete samples, which were immersed, with normal control, in the test-environment, while positive control samples were immersed in distilled water. Electrochemical measurements of corrosion-rate (by linear-polarization-resistance instrument), corrosion-current (by zero-resistance-ammeter) and corrosion-potential (by high impedance multimeter) were obtained for assessing the reinforcing-steel corrosion. Analyzed results showed that the corrosion-rate exhibited excellent correlation (R = 98.82%, Nash-Sutcliffe Efficiency = 97.66%, ANOVA p-value = 0.0006) with function of the admixture concentration and of the corrosion noise-resistance (ratio of corrosion-potential and corrosion-current standard deviations). The 0.3333% *Phyllanthus muellerianus* (per weight of cement) exhibited optimal efficiency, η = 97.58% $\pm$ 1.28% (experimental) or 95.33% $\pm$ 4.25% (predicted), at inhibiting concrete steel-reinforcement corrosion in the test-environment, which compares well with the positive control performance model, η = 97.96% $\pm$ 0.03%. The experimental and predicted models followed the Langmuir adsorption isotherm, which indicated physisorption as the *Phyllanthus muellerianus* leaf-extract adsorption mechanism on the reinforcing-steel. These support suitability of the N-, S-, and O-containing and π-electron rich *Phyllanthus muellerianus* leaf-extract as an environmentally-friendly inhibitor for effective corrosion-protection of steel-reinforcement in concrete designed for the saline/marine environment.

Keywords: steel-reinforcement corrosion; non-destructive tests by electrochemical corrosion monitoring; saline/marine simulating-environment; environmentally-friendly inhibitor; analyses of metallic corrosion test-data; inhibition of metallic corrosion; Langmuir adsorption isotherm

1. Introduction

Steel-reinforced concrete is a global material of choice for building structures and infrastructure, especially due to its relatively lower cost and the inherent protection of the reinforcing-steel embedment from environmental degradation within the concrete [1,2]. The reinforcing-steel (steel-rebar), in turn, improves the load-bearing strength properties of the concrete for the steel-reinforced concrete application. The inherent protection of steel-reinforcement in concrete takes the form of high alkalinity of concrete pore environment, usually of pH > 12, which promotes the development of a thin passive film of oxide layer on the reinforcing-steel surface [1,3–6]. However, destruction of the thin passive oxide layer, by penetrations of aggressive agents through the concrete, from its service-environment,

unto the steel-rebar, renders the rebar susceptible to corrosion degradation. Dominant, out of the many, environmental agents capable of promoting steel-rebar corrosion include ingress of chloride ions, in artificial saline from de-icing salts in temperate region, or in natural marine from seawater in coastal areas, into concrete unto the steel-rebar [2,7–11].

Steel-reinforced structures, usually in these chloride-contaminated environments, include: steel-reinforced energy structures, commercial or domiciliary buildings, tunnels, roads/pavements, bridges, storm barriers, wharfs, harbors, platforms, and man-made concrete islands [2,12–19]. The rusts produced by the ensuing corrosion degradation of the steel-reinforcement are expansive within the concrete such that they generate hoop stress that leads to cracks, spalling, delamination and loss of structural integrity of the steel-reinforced structure. Maintenance, rehabilitations and repairs, for averting catastrophic collapse of corrosion deteriorated steel-reinforced structures, constitute huge spending and substantial parts of fiscal budgetary allocations in many countries [17,18,20]. Otherwise, the insidious nature of chloride-induced corrosion failure of steel-reinforced concrete structures and infrastructures in saline/marine environment, if unchecked, could culminate in safety risks to life and/or loss of properties [21,22].

Despite many other corrosion-protection methods, the use of green, environmentally-friendly corrosion inhibiting admixtures, especially from natural plant materials, is attracting preference among researchers and construction stakeholders due to many advantages. Corrosion inhibiting substances from natural plant materials are of relatively lower cost due to their ready availability in the environment. They combine this desirable quality with being biodegradable, non-toxic and non-hazardous to the environmental ecosystem. These properties are unlike traditional synthetic chemical inhibitors, e.g., compounds of chromates and nitrites [23], which are known to be both toxic to the environment and capable of causing temporary or permanent damage to organs (e.g., kidneys and/or liver) of living beings [24,25]. Rather, corrosion inhibitors from natural plant sources are rich in biocompatible organic compounds that are able to exhibit corrosion-protection by adsorption on the metal-solution interface [26,27]. These naturally occurring substances can be safely extracted, synthesized, characterized and applied for the corrosion inhibition process using simple and standard procedures in contrasts to injurious chemicals and processes required for synthesizing traditional chemical inhibitors [26,28]. However, the fact that corrosion inhibitors are medium and/or material specific necessitates test on the corrosion inhibition property of the extract from specified plant on given metallic material, and in a given medium, of interest [29]. In a closely related consideration, substances that had exhibited positive inhibition effects on reinforcing-steel corrosion but in concrete pore solution are still recommended for further tests in physically cast concrete, in which they may require additional compatibility criteria [30–32].

Studies on biochemical characterization of *Phyllanthus muellerianus* (*P. muellerianus*) Euphorbiaceae leaf-extract showed that the plant is rich in lone-pairs and π-electron containing heteroatoms and biocompatible phytochemical constituents [33,34]. From those studies, phytochemical constituents found in *P. muellerianus* include tannins, flavonoids, phlobatannins, alkaloids, saponins, and terpernoids. According to further reports [34,35], *P. muellerianus* leaf-extract is non-toxic, rather, the leaf of this plant has been found suitable for medicinal purposes including potencies of deep wound healing and antiplasmodial (i.e., against malaria causing parasite) activities. Corrosion research works have also identified *P. muellerianus* leaf-extract as an effective inhibitor of steel-reinforcement corrosion in concrete for the industrial/microbial service-environment [33,36].

Special motivation for this work had been drawn from studies that had successfully employed leaf-extract from *Phyllanthus amarus* (a different plant but from the same Euphorbiaceae family [37] as *P. muellerianus*) for inhibiting steel corrosion in acidic sulfate and in chloride contaminated media [29,38]. However, there is a dearth of studies on the anticorrosion potential of *P. muellerianus* leaf-extract on reinforcing-steel in concrete for chloride contaminated medium. Therefore, the objective of this study was to investigate the effects of *P. muellerianus* leaf-extract on steel-reinforcement corrosion in concrete immersed in 3.5% NaCl, simulating saline/marine environment.

2. Materials and Methods

2.1. Experimental Materials

Steel-reinforced concrete slabs for the study were cast in duplicates of size 100 mm × 100 mm × 200 mm that contained similar concentrations of *P. muellerianus* leaf-extract admixture, and which had been obtained following details from studies [33,36]. Six variations of the *P. muellerianus* leaf-extract were employed as admixtures in the duplicated design of steel-reinforced concrete specimens for the saline/marine test-environment. For these, the leaf-extract concentrations ranged from 0% *P. muellerianus* for the control or normal samples (Ctrl) in increment of 0.0833% (per weight of cement for the concrete mixing) up to 0.4167% admixtures. In addition to these, another duplicate of steel-reinforced concrete specimen with 0% *P. muellerianus* admixture was employed as set of positive controls for immersion in distilled water environment (i.e., Ctrl in Water). This usage of positive control without admixture was to ascertain that the corrosion effects in the experimental samples for the saline/marine environment followed from the immersion of the samples in their test-environment rather than from any other environmental effects.

In each sample of steel-reinforced concrete slab, was embedded, during casting, 150 mm part of a 190 mm length by 12 mm diameter deformed steel-rebar, such that the remaining 40 mm protrusion could be used for electrochemical test connections. Prior to their embedment in the concrete samples, each of the steel rods had been subjected to surface preparations as per ASTM G109-99a [39]. The reinforcing-steel is composed of elements by weight percent (wt. %) that include: 0.273 C, 0.780 Mn, 0.403 Si, 0.240 Cu, 0.109 Ni, 0.142 Cr, 0.039 P, 0.037 S, 0.0083 Nb, 0.0086 Co, 0.0063 Sn, 0.0037 Ce, 0.0032 V, 0.016 Mo and the balance Fe.

2.2. Experimental Setup

The saline/marine test-environment into which the twelve samples of steel-reinforced concrete slabs, for corrosion testing in this environment, were longitudinally and partially immersed was constituted of 3.5% NaCl test-solutions in plastic bowls. This usage of 3.5% NaCl medium for the saline/marine environment followed practice in studies [40–42] as well as the identification from text of the 3.5% by weight as the typical content of salt in most seawater [19]. The remaining two samples for corrosion test in this study were the duplicate of Ctrl in Water samples that were also longitudinally immersed in plastic bowls but which contained distilled water. The diagrammatic and pictorial representation of this longitudinal immersion model of samples followed that which has been presented in [43,44].

From each of these fourteen samples, three different, non-destructive tests (NDT) of electrochemical measurements were obtained in five days for the first 40 days and in seven days interval for the next seven weeks. These totaled 89 days of electrochemical test-experiments. The NDT electrochemical tests to which the steel-reinforced concrete samples were subjected include:

1. Corrosion-potential (CP) measurements versus $Cu/CuSO_4$ electrode (CSE), Model 8-A, obtained from Tinker & Rasor® (San Bernardino, CA, USA), using a high impedance digital multimeter (MASTECH® instrument, Guangdong, China) [44], conforming to ASTM C876-91 R99 [45].
2. Corrosion-current (CC) measurements, versus CSE using zero resistance ammeter (ZRA), Model ZM3P obtained from Corrosion Service® (Markham, ON, Canada) [43,46–48].
3. Corrosion-rate (CR) measurements from linear polarization resistance using the three-electrode LPR Data Logger, Model MS1500L, obtained from Metal Samples® (Munford, AL, USA) [46,48], and that gave direct readout of CR in mpy unit. The three-electrode system by the instrument include a brass plate auxiliary electrode, a Ag/AgCl SCE reference electrode (EDT direct-ION®, Dover, UK) and the steel-reinforcement working electrode [40,49,50]. The LPR Data Logger instrument was connected to the steel-reinforced concrete specimen using typical electrochemical cell setup detailed in [26,51].

2.3. Initiation of Corrosion Test-Data Analyses—Statistical Distribution Fitting

As prescribed in ASTM G16-95 R04 [52], for avoiding grossly erroneous conclusion, analyses of the non-destructive electrochemical measurements of steel-reinforcement corrosion were initiated through fittings of the test-data to the Normal and Weibull distributions [51]. Compatibility of the dataset from each test-variable per sample was also investigated using the Kolmogorov-Smirnov goodness-of-fit test-techniques [53,54]. Measurements of central tendencies, μ, and measurements of dispersions, σ, for each of the distribution fittings of datasets were obtained by maximum likelihood estimation (MLE) procedures [55] which for the Normal distribution employs the well-known formula [51,56] for μ_{Normal} in Equation (1) and σ_{Normal} in Equation (2):

$$\mu_{Normal} = \frac{1}{n}\sum_{i=1}^{n} x_i \tag{1}$$

$$\sigma_{Normal} = \sqrt{\frac{1}{n-1}\sum_{i=1}^{n}(x_i - \mu)^2} \tag{2}$$

whereas for the Weibull distribution, it was required that the MLE procedures be applied for estimating the Weibull shape, *k*, and scale, *c*, parameters through the solution of the simultaneous Equations (3) and (4) given by [51,56,57]:

$$\frac{n}{\hat{k}} - n\ln(\hat{c}) + \sum_{i=1}^{n}\ln x_i - \sum_{i=1}^{n}\left(\frac{x_i}{c}\right)^{\hat{k}}\ln\left(\frac{x_i}{c}\right) = 0 \tag{3}$$

$$\hat{c} - \left\{\frac{1}{n}\sum_{i=1}^{n} x_i^{\hat{k}}\right\}^{\frac{1}{\hat{k}}} = 0 \tag{4}$$

From the unbiased estimated values of *k* and *c*, the Weibull mean ($\mu_{Weibull}$) and standard deviation ($\sigma_{Weibull}$) were then evaluated by the respective expression in Equations (5) and (6):

$$\mu_{Weibull} = c\Gamma\left(1 + \frac{1}{k}\right) \tag{5}$$

$$\sigma_{Weibull} = \sqrt{c^2\left\{\Gamma\left(1 + \frac{2}{k}\right) - \left[\Gamma\left(1 + \frac{1}{k}\right)^2\right]\right\}} \tag{6}$$

2.4. Corrosion Noise-Resistance (R_n) Analyses

Measurements of dispersion from the descriptive statistics that exhibited better compatibility with the scatter of the corrosion-potential and the corrosion-current test-data were used for modeling the corrosion noise-resistance [56,58,59]. This noise-resistance was modeled as the ratio of standard deviation of corrosion-potential (CP) to the standard deviation of corrosion-current (CC), using the formula in Equation (7):

$$R_n = \frac{\sigma_{CP}}{\sigma_{CC}} \tag{7}$$

2.5. Surface Coverage and Inhibition Efficiency Analyses

Measurements of central tendencies from the descriptive statistics that exhibited better compatibility with the scatter of CR test-data were used for modeling the surface coverage (θ) and inhibition efficiency (η) of *P. muellerianus* leaf-extract on the steel-reinforcement. These facilitated estimations of θ and η, for each admixed *P. muellerianus* concentration in concrete relative to the Ctrl sample, through the respective relationship in Equations (8) and (9) [60,61]:

$$\theta = \frac{CR_{\text{Ctrl sample}} - CR_{\text{Admixed sample}}}{CR_{\text{Ctrl sample}}} \quad (8)$$

$$\eta = \frac{CR_{\text{Ctrl sample}} - CR_{\text{Admixed sample}}}{CR_{\text{Ctrl sample}}} \times 100 \quad (9)$$

2.6. Adsorption Isotherm Modeling

The surface coverage θ was subjected to the fitting of Langmuir adsorption isotherm through Equation (10) [56,60,62–64]:

$$\frac{\varrho}{\theta} = \frac{1}{K_{\text{ads}}} + \varrho \quad (10)$$

In Equation (10), ϱ is the concentration of *P. muellerianus* leaf-extract admixed in concrete, and K_{ads} is the Langmuir equilibrium constant for the adsorption-desorption process. The K_{ads} estimation facilitated the modeling of the nature of *P. muellerianus* leaf-extract adsorption through use of the K_{ads} for the separation factor, R_{L}, computation in Equation (11) [56,60,65,66]:

$$R_{\text{L}} = \frac{1}{1 + K_{\text{ads}} C R_0} \quad (11)$$

The R_{L} computation, therefore, finds usefulness for indicating *P. muellerianus* leaf-extract adsorption on reinforcing-steel as irreversible if $R_{\text{L}} = 0$, or favorable if $0 < R_{\text{L}} < 1$, or linear if $R_{\text{L}} = 1$, or unfavorable if $R_{\text{L}} > 1$ [60,66]. In addition to these, the K_{ads} of the Langmuir isotherm model was used for estimating the Gibbs free energy of adsorption ΔG_{ads} using Equation (12) [56,60,62–64]:

$$\Delta G_{\text{ads}} = -2.303 RT \log (55.5 K_{\text{ads}}) \quad (12)$$

In Equation (12), R is the molar gas constant ≡ 8.314 J/mol·K, and T is the absolute temperature ≡ 300 K, while 55.5 represents the concentration of water in solution expressed in molar. Estimated value of Gibbs free energy of adsorption that is around or more positive than −20 kJ/mol suggests prevalent physisorption (or physical adsorption) mechanism, while estimated value that is around or more negative than −40 kJ/mol suggests prevalent chemisorption (or chemical adsorption) mechanism.

3. Results and Discussion

3.1. Statistical Distribution Fitting and Analyses of Corrosion Test-Variables

Figure 1 shows the mean plots, obtained from the statistical analyses of corrosion test-variables from each sample by the Normal and the Weibull distributions, for the corrosion potential Figure 1a, corrosion current Figure 1b and corrosion rate Figure 1c. The mean plots of corrosion potential and corrosion current, Figure 1a,b, also include the range of standard deviations for each of the datasets of these corrosion test-variables for each steel-reinforced concrete samples. In addition, and for aiding direct interpretations from the plotting, the plots of corrosion potential (Figure 1a) include linear plots of corrosion risk probability as per ASTM C876-91 R99 [45] while the plots of corrosion rate (Figure 1c) include a linear plot of typical corrosion rate criteria from literature [18,67].

From the plots in Figure 1, the general trend whereby corrosion test-variables of the normal control samples (Ctrl) were high-valued compared to the corrosion test-variables of samples admixed with *P. muellerianus* leaf-extract could be observed from each of the electrochemical tests. This general trend was such that values of the corrosion test-variables tend to range from the high-values for the Ctrl samples through reduced values for the samples with *P. muellerianus* down towards the low-values for the positive control samples that were immersed in water (Ctrl in Water). According to [68], the high values of CP test-variable, which classified to the severe corrosion risk region of [45], encountered in the Ctrl samples indicate prevalence of anodic (i.e., corroding) areas in the steel-rebar

embedment in the concentration cell of the 3.5% NaCl-immersed normal control concretes. By these, it could also be understood from [68] that the lower CP values obtained from the 3.5% NaCl-immersed concrete samples that were admixed with *P. muellerianus* suggest region whereby the plant extract promotes passive layer that enhances resistance of the steel-rebar to dissolution. In similar manner, and according to [69], the high CC values in the Ctrl samples gives the measure of the corrosion activity between the corroding anode, the steel-rebar in the samples, and the passive cathode of the Cu in the $Cu/CuSO_4$ reference electrode [68,69]. Therefore, the low values of CC obtained from the *P. muellerianus* admixed concretes also corroborate the low values of CP by the low CC values indicating low measure of corrosion activity between the steel-rebar in the concrete and the Cu in the reference electrode employed for this electrochemical test.

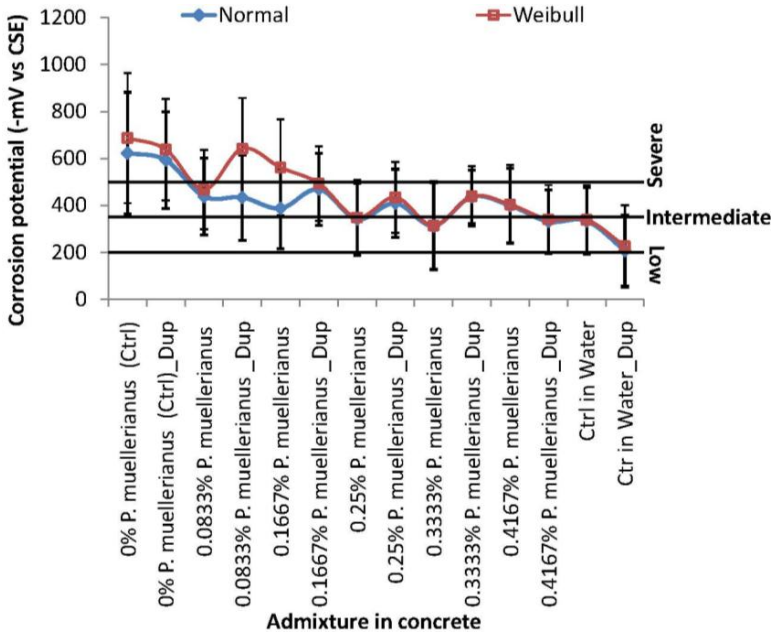

(**a**)

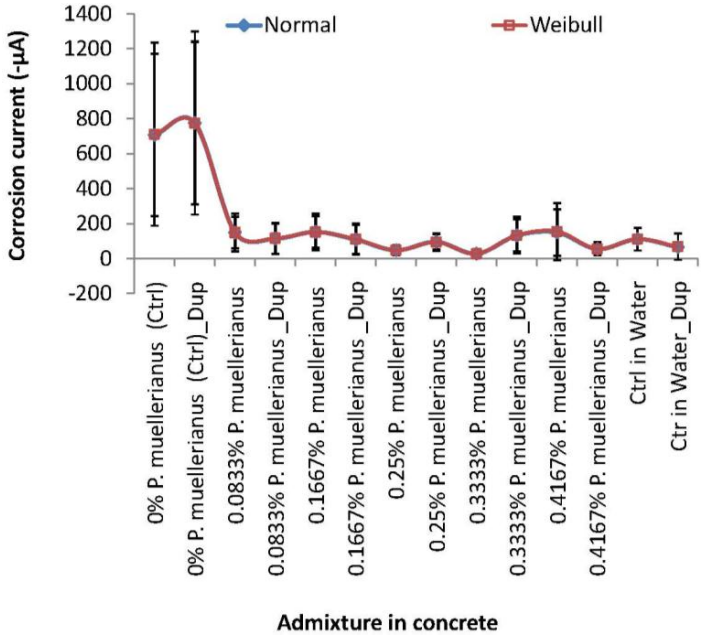

(**b**)

Figure 1. *Cont.*

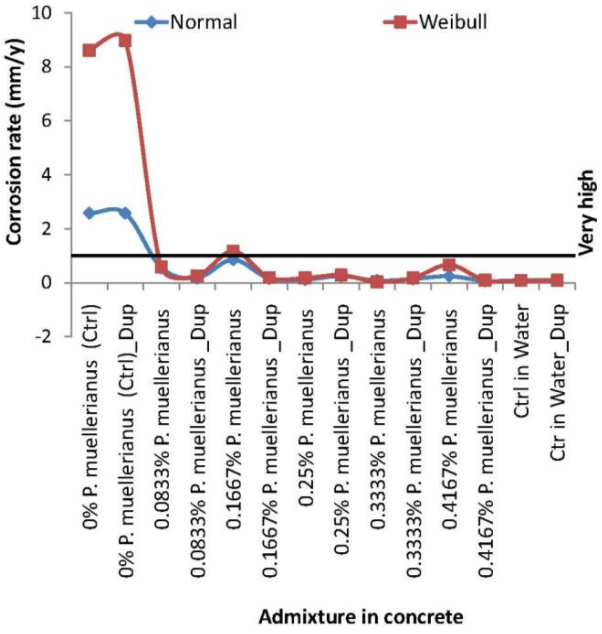

(**c**)

Figure 1. Statistical distribution analyses of corrosion test-variables: (**a**) mean ± standard deviation ranges of corrosion potential (CP) with linear plots of corrosion risks as per ASTM C876-91 R99 [45]; (**b**) mean ± standard deviation ranges of corrosion current (CC); and (**c**) mean corrosion rate (CR) with plot of classification of corrosion criteria as per [18,67].

In addition to these, and with just some few exceptions, especially in the corrosion potential plots of some samples, there were general agreements in the pattern of corrosion test-variable models by the Normal and by the Weibull distributions. However, the few over-predictions and discrepancies in model of corrosion test-variables necessitate investigation of the distribution that describes the scatter of the test-data from each corrosion test-variable better among the Normal and the Weibull distribution models.

Figure 2 therefore shows results of the Kolmogorov-Smirnov goodness-of-fit (K-S GoF) analyses of the scatter of the dataset of corrosion test-variables, from each sample of steel-reinforced concrete employed in this study, like the Normal and like the Weibull distribution. The plots in Figure 2 also include linear plot of $\alpha = 0.05$ level of significance for ascertaining analyzed dataset scattering like, or otherwise, each of the distribution fitting models. These showed that all the datasets of corrosion potential and of corrosion current scattered like both the Normal and the Weibull probability distributions according to the K-S GoF criteria at $\alpha = 0.05$ level of significance. However, datasets of corrosion rate from six steel-reinforced concrete samples, out of the 14 samples studied and which include datasets from the duplicates of normal control (Ctrl and Ctrl Dup), were not scattered like the Normal distribution. In contrast, all datasets of corrosion rate scattered like the Weibull distribution. These results indicate that while both the Normal and the Weibull distributions could be employed for describing the corrosion potential and the corrosion current, only the Weibull distribution, but not the Normal, could be used for describing the corrosion rate test-data.

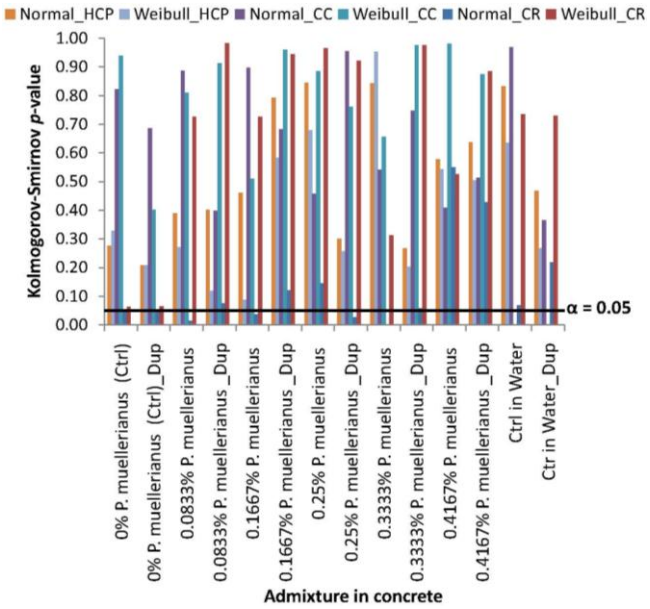

Figure 2. Kolmogorov-Smirnov goodness-of-fit test-results of the scatter of corrosion test data from the concrete samples like the Normal and the Weibull distributions.

3.2. Corrosion Rate and Corrosion Noise Resistance for Correlation Modeling

Based on the results from the K-S GoF analyses, the Weibull distribution model was employed in the study as the descriptive statistics for the corrosion test-variables. By these, the corrosion noise resistance, R_n, was also evaluated for each steel-reinforced concrete samples using ratios of Weibull model of standard deviations of corrosion potential to the standard deviations of corrosion current as per Equation (7). Figure 3, therefore, shows the results of the corrosion noise resistance for the steel-reinforced concrete samples, superimposed on the plots of corrosion rate, in increasing order of the corrosion rate effect on the embedded reinforcing-steel in the samples.

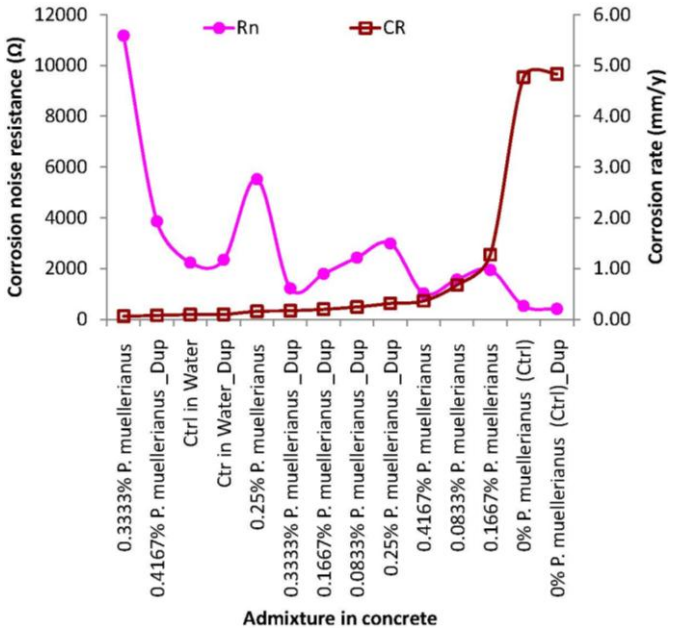

Figure 3. Plots of noise resistance and corrosion rate in ranking order of corrosion rate performance of *P. muellerianus* admixtures in concrete samples.

From this figure, it could be noted that the duplicate samples of normal Ctrl exhibited the lowest corrosion noise resistance as well as the highest corrosion rate in the experimental study. In addition, the 0.3333% *P. muellerianus* sample exhibited the highest corrosion noise resistance as well as the least corrosion rate in the study. This 0.3333% *P. muellerianus* sample and the 0.4167 *P. muellerianus*_Dup sample both exhibited higher corrosion noise resistance and lower corrosion rate than the values of these variables for the duplicate samples of "Ctrl in Water". Despite this, it is still worth noting that the duplicate samples of positive control, "Ctrl in Water" samples exhibited the kinds or agreements in corrosion rate effects that was exhibited by the duplicate samples of normal control, the Ctrl immersed in NaCl medium.

As could be observed in Figure 3, studies have shown that the corrosion noise resistance is generally high-valued at low corrosion rate and low-valued at high corrosion rate due to the fact that the corrosion noise resistance tracks the linear polarization resistance [36,56,59,60]. This relationship of corrosion noise resistance with corrosion rate, and vice versa, had been employed for detailing correlation expressions between these corrosion variables in reported works [36,56,60]. In a similar manner, it could be shown that the corrosion rate, CR, obtained from this study, exhibited relationship with the corrosion noise resistance, R_n, and the *P. muellerianus* leaf-extract admixture concentration, ϱ, which can be expressed in compact form as Equation (13):

$$\mathrm{CR} = 0.5057 \left[\varrho + \sum_{\lambda=0}^{5} (-1)^{\lambda+1} \cdot a_\lambda \cdot 10^{3\lambda} \cdot (1/R_n)^\lambda \right] \quad (13)$$

In Equation (13), values of the coefficients a_λ $\{\lambda = 0, 1, \ldots, 5\}$ are as presented in Table 1.

Table 1. Values of the coefficients a_λ in Equation (13).

λ	a_λ
0	0.6396
1	4.6268
2	29.3848
3	49.3821
4	31.1072
5	6.2572

For the correlation fitting expression in Equation (13), the correlation coefficient, R = 98.82% and the Nash-Sutcliffe efficiency, NSE = 97.66%, which interpret to excellent model fitting efficiency [70,71]. Analysis of variance for the correlation fitting expression (see Table 2) indicated that p-value = 0.0006, which implies that the correlated relationship between the dependent variable, CR, and the independent variables ϱ and R_n is statistically significant within 95% confidence interval.

Table 2. Analysis of variance for the correlation fitting expression in Equation (13).

Source of Variations	*df*	*SS*	*MS*	*F*	*p*-Value
Treatment	6	33.3438	5.5573	34.7807	0.0006
Residual	5	0.7989	0.1598		
Total	11	34.1428			

3.3. Corrosion Inhibition Effects by Experimental and Correlated Model

Plots of inhibition efficiency are presented in Figure 4, in ranking order of the *P. muellerianus* leaf-extract performance on concrete steel-reinforcement corrosion in the tested medium, using the experimental and the correlation predicted CR data applications to Equation (9). For further comparisons of corrosion effects, the figure also includes a linear plot of the analyzed corrosion rate

reduction effect from the positive control ("Ctrl in Water"), idealized as inhibition efficiency relative to the normal control (Ctrl), through use of Equation (9). By these, therefore, it could be deduced from the figure that the *P. muellerianus* leaf-extract concentrations effectively inhibited steel-reinforcement corrosion in concrete immersed in the chloride contaminated environment. However, in addition to these, the inhibition efficiency performance of the *P. muellerianus* leaf-extract concentrations tended towards that of the "Ctrl in Water" by both the experimental and the predicted models of corrosion. Thus, while the 0.3333% *P. muellerianus* leaf-extract exhibited optimal inhibition efficiency, $\eta = 97.58\% \pm 1.28\%$ (experimental) or $95.33\% \pm 4.25\%$ (predicted), this inhibition effect ranged towards that of the idealized inhibition efficiency, $\eta = 97.96\% \pm 0.03\%$, by the "Ctrl in Water".

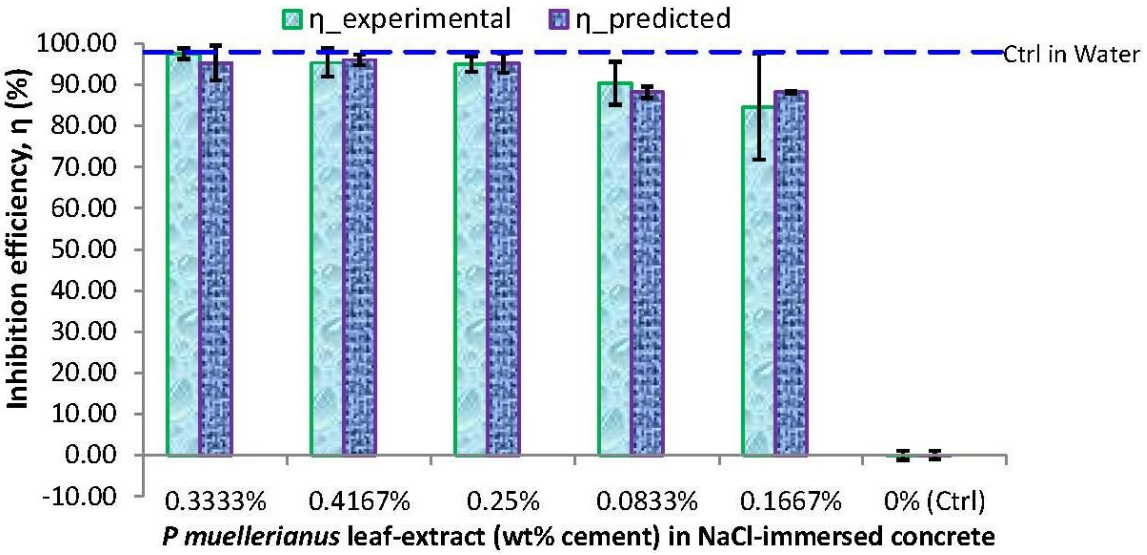

Figure 4. Ranking order of Inhibition efficiency performance by *P. muellerianus* leaf-extract.

The high range of idealized inhibition effects by the positive control samples laid credence to the fact that the corrosion effects from the normal controls followed from the immersion of the normal control samples in the saline/marine environment and not from any other effects. It is also worth noting that the optimal inhibition efficiency in this study by the 0.3333% *P. muellerianus* leaf-extract concentration finds similarity with the performance from previous work [36] by this same concentration on steel-reinforcement corrosion in H_2SO_4-immersed concrete. This performance was despite the longer experimental period of steel-reinforced concrete immersion in the chloride induced corrosive test-medium in this study. Rather, the inhibition performance by the 0.3333% *P. muellerianus* leaf-extract in the chloride contaminated medium in this study still surpassed that of the same admixture concentration in that acidic sulfate immersed medium. In addition to these, almost all concentrations of *P. muellerianus* leaf-extract inhibitors in this study exhibited excellent model, $\eta > 90\%$ of inhibition efficiencies both by the experimental and the correlation prediction models. The 0.16667% *P. muellerianus* leaf-extract admixture concentration modeled with the least inhibition efficiency of $\eta = 84.65\% \pm 12.88\%$ (experimental) or $88.22\% \pm 0.26\%$ (predicted) in this study indicates positive as well as "very good" efficiency model [70,71]. These exhibited further contrasts with results from that previous work whereby insufficient amount of *P. muellerianus* leaf-extract admixture exhibited negative inhibition effect (i.e., promotes corrosion aggravation) on steel-reinforcement corrosion in the H_2SO_4-immersed concrete.

3.4. Adsorption Isotherm Model of Experimental and Correlated Data

Figure 5 shows plots of the results obtained from fitting the experimental and the correlated predicted data to the Langmuir adsorption isotherm, through requisite applications of Equations (8)

and (10), while Table 3 presents the adsorption fitting parameters. In the figure, the ratio of *P. muellerianus* concentration to the surface coverage model (ϱ/θ) was plotted, as the ordinate, against the concentration (ϱ) of the plant extract, as the abscissa, for obtaining the intercept $1/K_{ads}$, the reciprocal of the Langmuir equilibrium constant, as per Equation (10). Figure 5 shows that both the experimental and correlation predicted data linearly fit the Langmuir adsorption isotherm model, which by their $R > 99\%$ correlation coefficients, as tabulated, interpret also to excellent isotherm modeling efficiency. The values of the separation factor that were in the range $0 < R_L < 1$ indicate favorable adsorption [60,66] by the *P. muellerianus* leaf-extract inhibitor on the concrete steel-reinforcement. In addition, the negative values of Gibbs free energy of adsorption indicate spontaneity of the *P. muellerianus* leaf-extract adsorption while the values of the parameter around −20 kJ/mol imply prevalent physisorption as the mechanism of *P. muellerianus* leaf-extract adsorption on the reinforcing-steel surface.

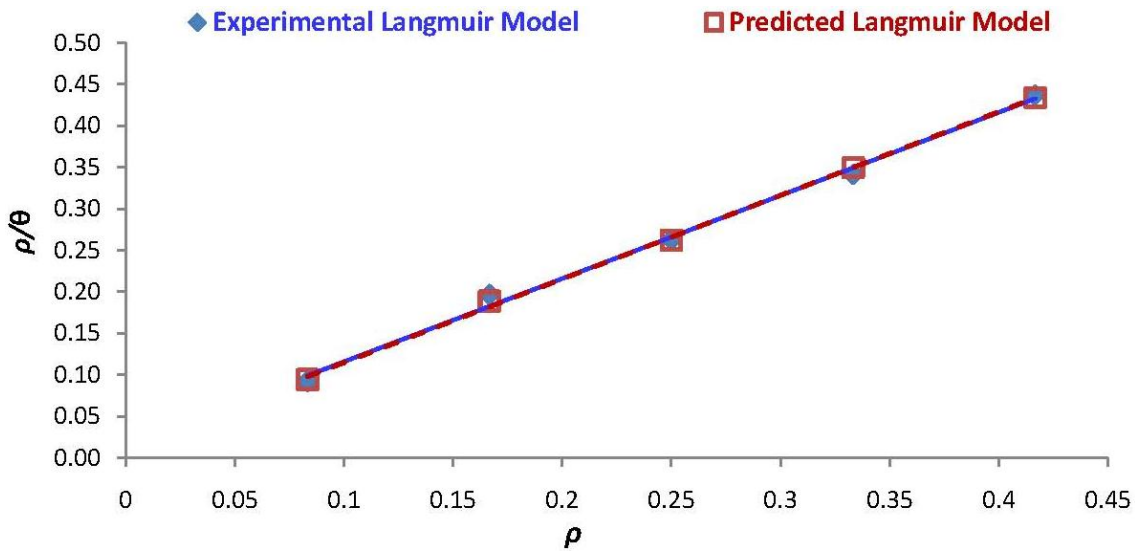

Figure 5. Plots of Langmuir adsorption isotherm fittings of experimental and correlation predicted performance of *P. muellerianus* leaf-extract on steel-reinforcement corrosion in the chloride contaminated environment.

Table 3. Parameters from Langmuir adsorption isotherm fitting of corrosion data.

Isotherm Parameter	Experimental Model	Predicted Model
K_{ads}	62.9422	71.1493
R, correlation coefficient, (%)	99.51	99.90
R_L, separation factor	3.2995×10^{-3}	2.9192×10^{-3}
ΔG_{ads} Gibbs free energy (kJ/mol)	–20.3492	–20.6549

The results from the study showed *P. muellerianus* leaf-extract as an effective environmentally-friendly inhibitor of steel-reinforcement corrosion in steel-reinforced concrete immersed in 3.5% NaCl test-environment, for representing saline/marine environment. This inhibition effectiveness of the natural plant extract on steel-rebar corrosion in the chloride contaminated medium could be due to its constituents of lone pair and π-electrons rich organic hetero-atoms that had shown positive inhibition prospects in acidic environment in previous studies.

3.5. Organic Bio-Constituent Model from P. muellerianus Leaf-Extract

The effectiveness of *P. muellerianus* leaf-extract on the corrosion protection of reinforcing steel in the chloride contaminated medium engender interest in the bio-constituent model that could be

available in the leaf-extract of the natural plant [56]. For this, the spectrum obtained from the Fourier Transform Infrared (FT-IR) spectroscopy instrument, the Perkin-Elmer® FT-IR System (Spectrum BX, Waltman, MA, USA), application to the *P. muellerianus* leaf-extract is presented in Figure 6.

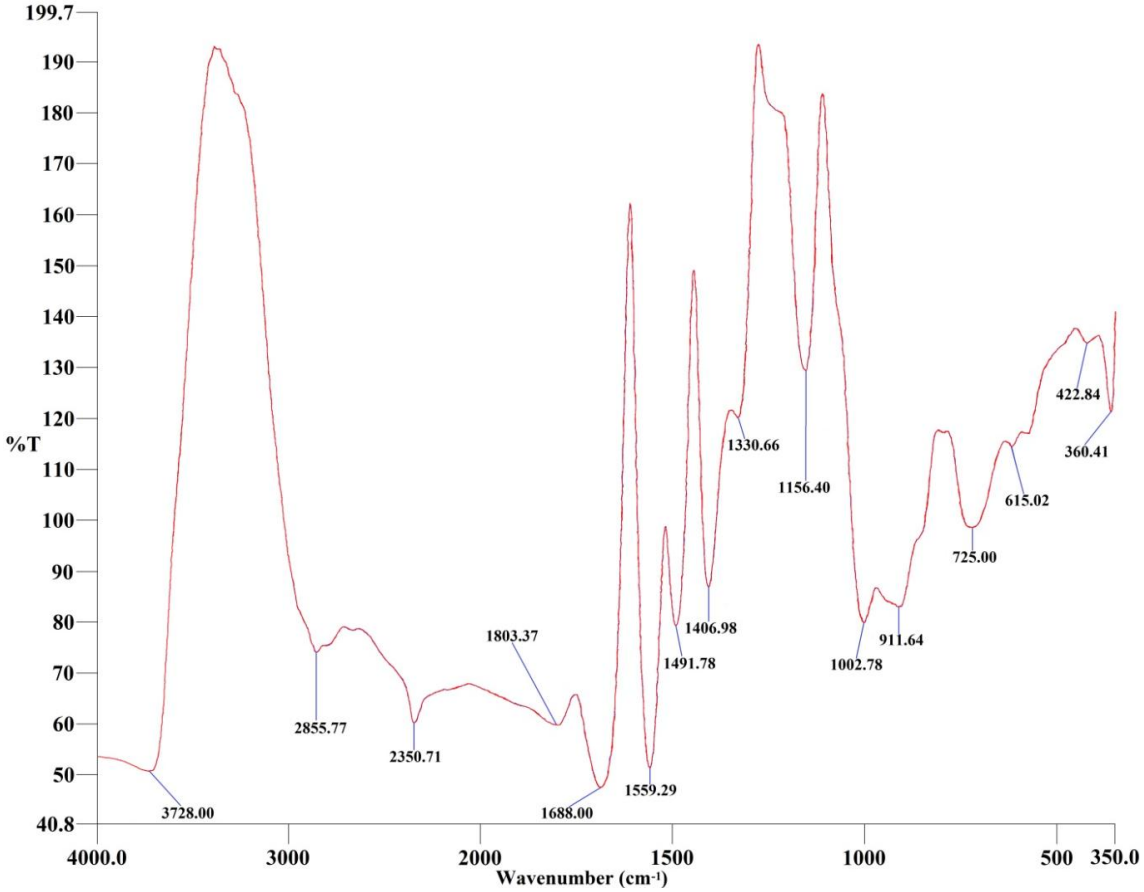

Figure 6. Fourier Transform Infrared (FT-IR) spectrum of *P. muellerianus* leaf-extract.

As had been previously detailed, the functional classes of adsorbed vibrations, for the identified frequencies in the *P. muellerianus* leaf-extract FT-IR spectrum (Figure 6), had been reported, along with the phytochemical characterization, by [33]. However, the rendering of this FT-IR spectrum to the Euclidean Search of the Fluka library, by the Perkin-Elmer® instrument [72], suggested hit list of 10 organic compounds that are presented, in this study, as 3-D optimized structures of the compounds in Figure 7.

Figure 7 shows that, out of the 10 compounds identified in the *P. muellerianus* leaf-extract spectrum, eight contain aromatic rings, seven are N- (nitrogen), two are S- (sulfur), one is Br- (bromine) and seven are O- (oxygen) containing lone-pair and/or π-electrons rich organic compounds. In addition, it is worth noting that five of the identified compounds for *P. muellerianus* find similarities to those that were identified for *Morinda lucida* in [72] while the remaining five were not found in *Morinda lucida* but in *P. muellerianus* leaf-extract. In this study, however, *P. muellerianus* leaf-extract concentrations exhibited high effectiveness performance, which compares well to that obtained from positive (distilled water immersed) control samples, on the inhibition of steel-reinforcement corrosion in concrete for the saline/marine simulating environment. This performance was in similar manner with that by the *P. muellerianus* for the industrial/microbial environment in [36], and with that obtained by the also N-, S-, and O-containing *Morinda lucida* for the saline/marine environment in [72]. The corrosion inhibition effects by these natural plant-extracts find agreements with what obtained in reported works [73–76], where effective corrosion inhibition of steel material in acidic environments had been observed with

uses of N-, S-, and O-containing and π-electron rich chemical derivatives. These considerations, therefore, also garner further support for the usage of the N-, S-, and O-containing and π-electron rich *P. muellerianus* leaf-extract as an environmentally-friendly inhibitor of steel-reinforcement corrosion in concrete designed for the saline/marine environment.

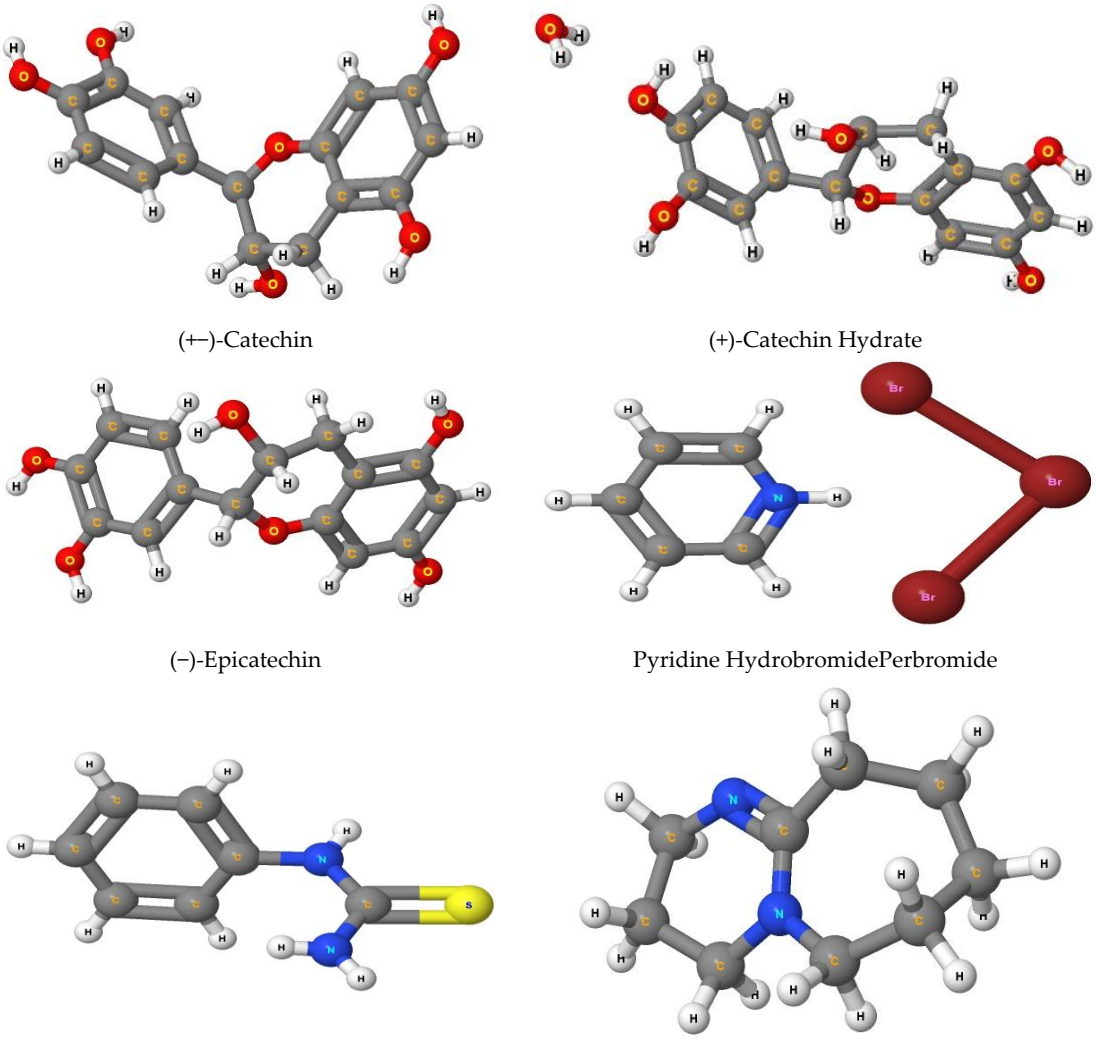

(+−)-Catechin

(+)-Catechin Hydrate

(−)-Epicatechin

Pyridine HydrobromidePerbromide

N-Phenylthiourea

1,8-Diazabicyclo[5.4.0]undec-7-ene

Figure 7. *Cont.*

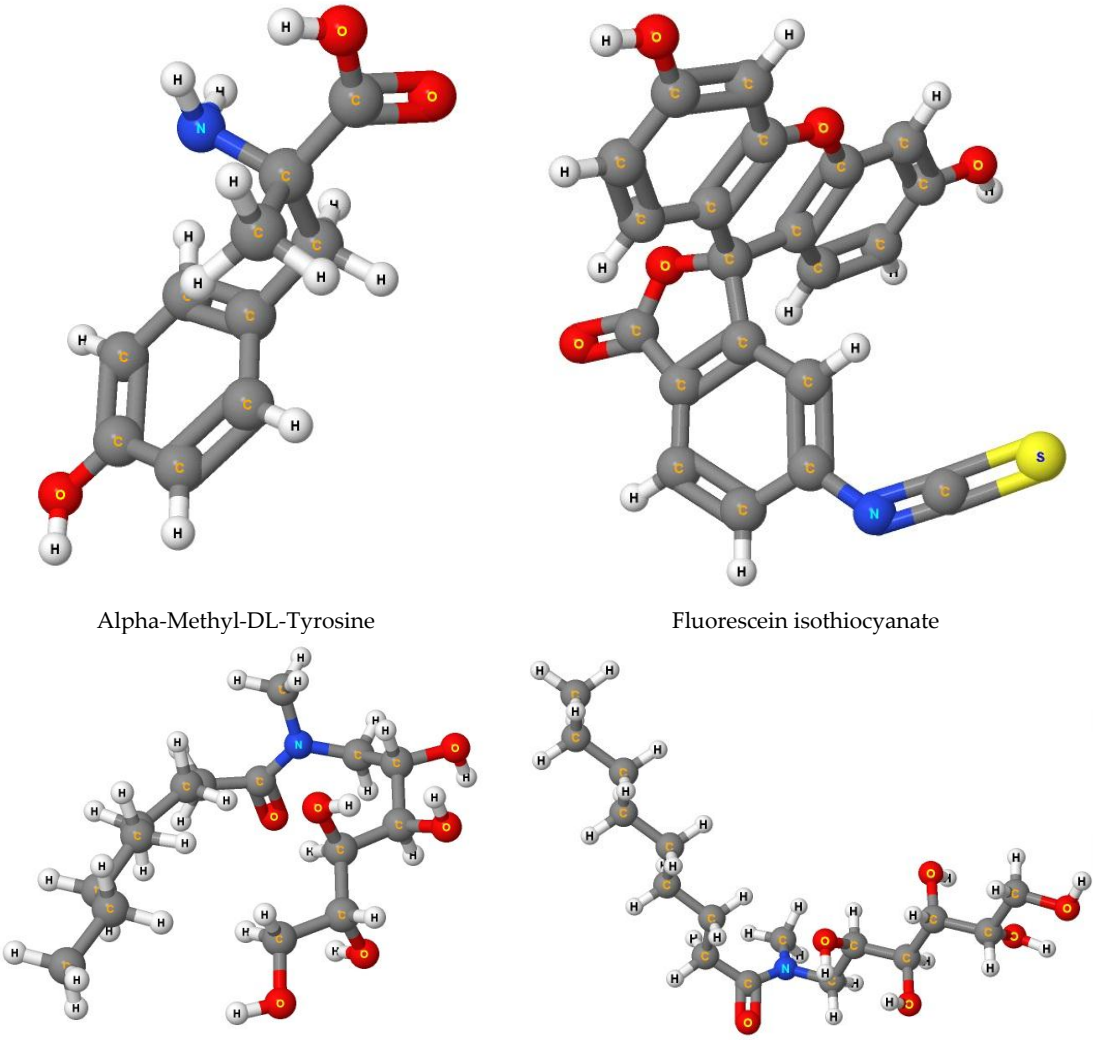

Figure 7. 3-D Optimized structures of organic compounds from the Euclidean Search hit-list of *P. muellerianus* leaf-extract FT-IR spectrum.

4. Conclusions

Anticorrosion effects of *P. muellerianus* leaf-extract on steel-reinforcement in concrete immersed in 3.5% NaCl, for simulating saline/marine environment, was investigated, in an experimental design employing normal control (in tested medium) and positive control (in distilled water). Statistical analyses of the experimental data identified the Weibull distribution as the descriptive statistics of better-fit for the corrosion test-data, according to the Kolmogorov–Smirnov goodness-of-fit criteria. Analyzed results showed that the corrosion rate from LPR instrument exhibited excellent correlation (R = 98.82%, Nash–Sutcliffe Efficiency = 97.66%, ANOVA p-value = 0.0006) with function of the *P. muellerianus* leaf-extract concentration and of the corrosion noise-resistance.

The 0.3333% *P. muellerianus* leaf-extract admixture (per weight of cement) exhibited optimal inhibition efficiency, η = 97.58% $\pm$ 1.28% (experimental) or 95.33% $\pm$ 4.25% (predicted), on steel-reinforcement corrosion in concrete samples immersed in the saline/marine test-environment. These results of corrosion inhibition effectiveness from the *P. muellerianus* leaf-extract admixtures compare well with the performance model, η = 97.96% $\pm$ 0.03%, of corrosion test-results obtained from the positive (i.e., the distilled water immersed) control samples. Subjection of the experimental and correlation predicted data to adsorption isotherm modeling indicated they both followed the

Langmuir adsorption isotherm. This isotherm model identified spontaneous/favorable adsorption and prevalent physisorption as the mechanism of *P. muellerianus* leaf-extract on the corrosion-protection of the reinforcing-steel in the concrete for the saline/marine environment.

These performances support suitability of the N-, S-, O-containing and π-electron rich *P. muellerianus* leaf-extract, as indicated from Euclidean Search Hit List application to the FT-IR spectrum of the plant extract, as an environmentally-friendly corrosion inhibitor. Usage of the extract from this natural plant is therefore recommended for effective corrosion-protection of steel-reinforcement in concrete designed for the saline/marine environment.

Acknowledgments: J.O.O. wishes to acknowledge and appreciate the assistance and supports received from the Department of Civil Engineering and the Department of Building Technology in Covenant University, Ota, Nigeria. From these departments requisite equipment and facilities were obtained for the standard casting and curing of concrete samples employed for the experiments in this research work.

Author Contributions: J.O.O. designed and conducted the experiments with the supervisory assistance and valuable recommendations on the research work by C.A.L. and A.P.I.P. C.A.L. and A.P.I.P. examined and assisted in the validation and interpretation of the experimental data. J.O.O. performed the experimental data analysis. All authors have contributed to discussing, documenting and reporting of the article script.

Conflicts of Interest: The authors declare no conflicts of interest.

References

1. Yang, Z.; Fischer, H.; Polder, R. Laboratory investigation of the influence of two types of modified hydrotalcites on chloride ingress into cement mortar. *Cem. Concr. Compos.* **2015**, *58*, 105–113. [CrossRef]
2. Rosas, O.; Maya-Visuet, E.; Castaneda, H. Effect of chloride ions on the electrochemical performance of LDX 2003 alloy in concrete and simulated concrete-pore solutions. *J. Appl. Electrochem.* **2014**, *44*, 631–646. [CrossRef]
3. Okeniyi, J.O. $C_{10}H_{18}N_2Na_2O_{10}$ inhibition and adsorption mechanism on concrete steel-reinforcement corrosion in corrosive environments. *J. Assoc. Arab Univ. Basic Appl. Sci.* **2016**, *20*, 39–48. [CrossRef]
4. Hu, J.; Koleva, D.A.; van Breugel, K. Corrosion performance of reinforced mortar in the presence of polymeric nano-aggregates: Electrochemical behavior, surface analysis, and properties of the steel/cement paste interface. *J. Mater. Sci.* **2012**, *47*, 4981–4995. [CrossRef]
5. Garcés, P.; Saura, P.; Zornoza, E.; Andrade, C. Influence of pH on the nitrite corrosion inhibition of reinforcing steel in simulated concrete pore solution. *Corros. Sci.* **2011**, *53*, 3991–4000. [CrossRef]
6. Tam, C.T.; Lim, H.B.; Sisomphon, K. Carbonation of concrete in the tropical environment of Singapore. *IES J. Part A Civ. Struct. Eng.* **2008**, *1*, 146–153. [CrossRef]
7. Zhu, X.; Zi, G.; Cao, Z.; Cheng, X. Combined effect of carbonation and chloride ingress in concrete. *Constr. Build. Mater.* **2016**, *110*, 369–380. [CrossRef]
8. Faustino, P.; Brás, A.; Ripper, T. The effect of corrosion inhibitors on the modelling of design lifetime of RC structures. *Mater. Struct.* **2015**, *48*, 1303–1319. [CrossRef]
9. Okeniyi, J.O.; Loto, C.A.; Popoola, A.P.I. Corrosion inhibition of concrete steel-reinforcement in saline/marine simulating-environment by *Rhizophora mangle* L. *Solid State Phenom.* **2015**, *227*, 185–189. [CrossRef]
10. Muthulingam, S.; Rao, B.N. Non-uniform time-to-corrosion initiation in steel reinforced concrete under chloride environment. *Corros. Sci.* **2014**, *82*, 304–315. [CrossRef]
11. Rakanta, E.; Daflou, E.; Batis, G. Evaluation of organic corrosion inhibitor effectiveness into the concrete. In *Measuring, Monitoring and Modeling Concrete Properties*; Konsta-Gdoutos, M.S., Ed.; Springer: Dordrecht, The Netherlands, 2006; pp. 605–611.
12. Pang, L.; Li, Q. Service life prediction of RC structures in marine environment using long term chloride ingress data: Comparison between exposure trials and real structure surveys. *Constr. Build. Mater.* **2016**, *113*, 979–987. [CrossRef]
13. Okeniyi, J.O.; Loto, C.A.; Popoola, A.P.I. *Morinda lucida* effects on steel-reinforced concrete in 3.5% NaCl: Implications for corrosion-protection of wind-energy structures in saline/marine environments. *Energy Proced.* **2014**, *50*, 421–428. [CrossRef]
14. Biondini, F.; Camnasio, E.; Palermo, A. Lifetime seismic performance of concrete bridges exposed to corrosion. *Struct. Infrastruct. Eng.* **2014**, *10*, 880–900. [CrossRef]

15. Boero, J.; Schoefs, F.; Yáñez-Godoy, H.; Capra, B. Time-function reliability of harbour infrastructures from stochastic modelling of corrosion. *Eur. J. Environ. Civ. Eng.* **2012**, *16*, 1187–1201. [CrossRef]
16. Pakrashi, V.; Schoefs, F.; Memet, J.B.; O'Connor, A. ROC dependent event isolation method for image processing based assessment of corroded harbour structures. *Struct. Infrastruct. Eng.* **2010**, *6*, 365–378. [CrossRef]
17. Cusson, D.; Qian, S.; Chagnon, N.; Baldock, B. Corrosion-inhibiting systems for durable concrete bridges. I: Five-year field performance evaluation. *J. Mater. Civ. Eng.* **2008**, *20*, 20–28. [CrossRef]
18. Söylev, T.A.; McNally, C.; Richardson, M. Effectiveness of amino alcohol-based surface-applied corrosion inhibitors in chloride-contaminated concrete. *Cem. Concr. Res.* **2007**, *37*, 972–977. [CrossRef]
19. Mehta, P.K. *Concrete in the Marine Environment*; CRC Press: New York, NY, USA, 2002.
20. Yousif, H.A.; Al-Hadeethi, F.F.; Al-Nabilsy, B.; Abdelhadi, A.N. Corrosion of steel in high-strength self-compacting concrete exposed to saline environment. *Int. J. Corros.* **2014**, *2014*, 1–11. [CrossRef]
21. Tarighat, A.; Zehtab, B. Structural reliability of reinforced concrete beams/columns under simultaneous static loads and steel reinforcement corrosion. *Arab. J. Sci. Eng.* **2016**. [CrossRef]
22. Budelmann, H.; Holst, A.; Wichmann, H.J. Non-destructive measurement toolkit for corrosion monitoring and fracture detection of bridge tendons. *Struct. Infrastruct. Eng.* **2014**, *10*, 492–507. [CrossRef]
23. Omotosho, O.A.; Okeniyi, J.O.; Ajayi, O.O.; Loto, C.A. Effect of synergies of $K_2Cr_2O_7$, K_2CrO_4, $NaNO_2$ and aniline inhibitors on the corrosion potential response of steel reinforced concrete in saline medium. *Int. J. Environ. Sci.* **2012**, *2*, 2346–2259.
24. Asipita, S.A.; Ismail, M.; Majid, M.Z.; Majid, Z.A.; Abdullah, C.; Mirza, J. Green *Bambusa arundinacea* leaves extract as a sustainable corrosion inhibitor in steel reinforced concrete. *J. Clean Prod.* **2014**, *67*, 139–146. [CrossRef]
25. Patel, N.S.; Jauhariand, S.; Mehta, G.N.; Al-Deyab, S.S.; Warad, I.; Hammouti, B. Mild steel corrosion inhibition by various plant extracts in 0.5 M sulphuric acid. *Int. J. Electrochem. Sci.* **2013**, *8*, 2635–2655.
26. Ismail, M.; Raja, P.B.; Salawu, A.A. Developing deeper understanding of green inhibitors for corrosion of reinforcing steel in concrete. In *Handbook of Research on Recent Developments in Materials Science and Corrosion Engineering Education*; Lim, H.L., Ed.; IGI Global: Hershey, PA, USA, 2015; pp. 118–146. [CrossRef]
27. Khan, G.; Newaz, K.M.; Basirun, W.J.; Ali, H.B.; Faraj, F.L.; Khan, G.M. Application of natural product extracts as green corrosion inhibitors for metals and alloys in acid pickling processes—A review. *Int. J. Electrochem. Sci.* **2015**, *10*, 6120–6134.
28. Abdulrahman, A.S.; Ismail, M.; Hussain, M.S. Corrosion inhibitors for steel reinforcement in concrete: A review. *Sci. Res. Essays* **2011**, *6*, 4152–4162. [CrossRef]
29. Okafor, P.C.; Ikpi, M.E.; Uwah, I.E.; Ebenso, E.E.; Ekpe, U.J.; Umoren, S.A. Inhibitory action of *Phyllanthus amarus* extracts on the corrosion of mild steel in acidic media. *Corros. Sci.* **2008**, *50*, 2310–2317. [CrossRef]
30. Etteyeb, N.; Dhouibi, L.; Takenouti, H.; Triki, E. Protection of reinforcement steel corrosion by phenyl phosphonic acid pre-treatment PART I: Tests in solutions simulating the electrolyte in the pores of fresh concrete. *Cem. Concr. Compos.* **2015**, *55*, 241–249. [CrossRef]
31. Ormellese, M.; Lazzari, L.; Goidanich, S.; Fumagalli, G.; Brenna, A. A study of organic substances as inhibitors for chloride-induced corrosion in concrete. *Corros. Sci.* **2009**, *51*, 2959–2968. [CrossRef]
32. Etteyeb, N.; Dhouibi, L.; Sanchez, M.; Alonso, C.; Andrade, C.; Triki, E. Electrochemical study of corrosion inhibition of steel reinforcement in alkaline solutions containing phosphates based components. *J. Mater. Sci.* **2007**, *42*, 4721–4730. [CrossRef]
33. Okeniyi, J.O.; Omotosho, O.A.; Ogunlana, O.O.; Okeniyi, E.T.; Owoeye, T.F.; Ogbiye, A.S.; Ogunlana, E.O. Investigating prospects of *Phyllanthus muellerianus* as eco-friendly/sustainable material for reducing concrete steel-reinforcement corrosion in industrial/microbial environment. *Energy Proced.* **2015**, *74*, 1274–1281. [CrossRef]
34. Agyare, C.; Lechtenberg, M.; Deters, A.; Petereit, F.; Hensel, A. Ellagitannins from *Phyllanthus muellerianus* (Kuntze) Exell.: Geraniin and furosin stimulate cellular activity, differentiation and collagen synthesis of human skin keratinocytes and dermal fibroblasts. *Phytomedicine* **2011**, *18*, 617–624. [CrossRef] [PubMed]
35. Zirihi, G.N.; Mambu, L.; Guédé-Guina, F.; Bodo, B.; Grellier, P. In vitro antiplasmodial activity and cytotoxicity of 33 West African plants used for treatment of malaria. *J. Ethnopharmacol.* **2005**, *98*, 281–285. [CrossRef] [PubMed]

36. Okeniyi, J.O.; Loto, C.A.; Popoola, A.P.I. Electrochemical performance of *Phyllanthus muellerianus* on the corrosion of concrete steel-reinforcement in industrial/microbial simulating-environment. *Port. Electrochim. Acta* **2014**, *32*, 199–211. [CrossRef]
37. Patel, J.R.; Tripathi, P.; Sharma, V.; Chauhan, N.S.; Dixit, V.K. *Phyllanthus amarus*: Ethnomedicinal uses, phytochemistry and pharmacology: A review. *J. Ethnopharmacol.* **2011**, *138*, 286–313. [CrossRef] [PubMed]
38. Sangeetha, M.; Rajendran, S.; Sathiyabama, J.; Krishnaveni, A.; Shanthy, P.; Manimaran, N.; Shyamaladevi, B. Corrosion inhibition by an aqueous extract of *Phyllanthus amarus*. *Port. Electrochim. Acta* **2011**, *29*, 429–444. [CrossRef]
39. ASTM G109-99a. *Standard Test Method for Determining the Effects of Chemical Admixtures on the Corrosion of Embedded Steel Reinforcement in Concrete Exposed to Chloride Environments*; ASTM International: West Conshohocken, PA, USA, 2005.
40. Yang, Y.; Scantlebury, J.D.; Koroleva, E.V. A study of calcareous deposits on cathodically protected mild steel in artificial seawater. *Metals* **2015**, *5*, 439–456. [CrossRef]
41. Zafeiropoulou, T.; Rakanta, E.; Batis, G. Performance evaluation of organic coatings against corrosion in reinforced cement mortars. *Prog. Org. Coat.* **2011**, *72*, 175–180. [CrossRef]
42. Mennucci, M.M.; Banczek, E.P.; Rodrigues, P.R.; Costa, I. Evaluation of benzotriazole as corrosion inhibitor for carbon steel in simulated pore solution. *Cem. Concr. Compos.* **2009**, *31*, 418–424. [CrossRef]
43. Okeniyi, J.O.; Loto, C.A.; Popoola, A.P.I. Anticorrosion performance of *Anthocleista djalonensis* on steel-reinforced concrete in a sulphuric-acid medium. *HKIE Trans.* **2016**. [CrossRef]
44. Okeniyi, J.O.; Omotosho, O.A.; Ajayi, O.O.; Loto, C.A. Effect of potassium-chromate and sodium-nitrite on concrete steel-rebar degradation in sulphate and saline media. *Constr. Build. Mater.* **2014**, *50*, 448–456. [CrossRef]
45. ASTM C876-91 R99. *Standard Test Method for Half-Cell Potentials of Uncoated Reinforcing Steel in Concrete*; ASTM International: West Conshohocken, PA, USA, 2005.
46. Okeniyi, J.O.; Omoniyi, O.M.; Okpala, S.O.; Loto, C.A.; Popoola, A.P.I. Effect of ethylenediaminetetraacetic disodium dihydrate and sodium nitrite admixtures on steel-rebar corrosion in concrete. *Eur. J. Environ. Civ. Eng.* **2013**, *17*, 398–416. [CrossRef]
47. Abdelaziz, G.E.; Abdelalim, A.M.; Fawzy, Y.A. Evaluation of the short and long-term efficiencies of electro-chemical chloride extraction. *Cem. Concr. Res.* **2009**, *39*, 727–732. [CrossRef]
48. Sastri, V.S. *Green Corrosion Inhibitors, Theory and Practice*; John Wiley & Sons: Hoboken, NJ, USA, 2011.
49. Okeniyi, J.O.; Oladele, I.O.; Omoniyi, O.M.; Loto, C.A.; Popoola, A.P.I. Inhibition and compressive-strength performance of $Na_2Cr_2O_7$ and $C_{10}H_{14}N_2Na_2O_8{\cdot}2H_2O$ in steel-reinforced concrete in corrosive environments. *Can. J. Civ. Eng.* **2015**, *42*, 408–416. [CrossRef]
50. Silaimani, S.M.; Vivekanandan, G.; Veeramani, P. Nano-nickel-copper alloy deposit for improved corrosion resistance in marine environment. *Int. J. Environ. Sci. Technol.* **2015**, *12*, 2299–2306. [CrossRef]
51. Okeniyi, J.O.; Ambrose, I.J.; Okpala, S.O.; Omoniyi, O.M.; Oladele, I.O.; Loto, C.A.; Popoola, P.A.I. Probability density fittings of corrosion test-data: Implications on $C_6H_{15}NO_3$ effectiveness on concrete steel-rebar corrosion. *Sadhana* **2014**, *39*, 731–764. [CrossRef]
52. ASTM G16-95 R04. *Standard Guide for Applying Statistics to Analysis of Corrosion Data*; ASTM International: West Conshohocken, PA, USA, 2005.
53. Okeniyi, J.O.; Okeniyi, E.T.; Atayero, A.A. Programming development of Kolmogorov-Smirnov goodness-of-fit testing of data normality as a Microsoft Excel® library function. *J. Softw. Syst. Dev.* **2015**. [CrossRef]
54. Okeniyi, J.O.; Okeniyi, E.T. Implementation of Kolmogorov-Smirnov *p*-value computation in Visual Basic®: Implication for Microsoft Excel® library function. *J. Stat. Comput. Simul.* **2012**, *82*, 1727–1741. [CrossRef]
55. Pham, H. Basic statistical concepts. In *Springer Handbook of Engineering Statistics*; Pham, H., Ed.; Springer-Verlag: London, UK, 2006; pp. 3–48.
56. Okeniyi, J.O.; Loto, C.A.; Popoola, A.P.I. Electrochemical performance of *Anthocleista djalonensis* on steel-reinforcement corrosion in concrete immersed in saline/marine simulating-environment. *Trans. Indian Inst. Met.* **2014**, *67*, 959–969. [CrossRef]
57. Lai, C.D.; Pra Murthy, D.N.; Xie, M. Weibull distributions and their applications. In *Springer Handbook of Engineering Statistics*; Pham, H., Ed.; Springer-Verlag: London, UK, 2006; pp. 63–78.

58. Eden, D.A. Electrochemical noise. In *Uhlig's Corrosion Handbook*, 2nd ed.; Revie, R.W., Ed.; Wiley: New York, NY, USA, 2000; pp. 1227–1238.
59. Kelly, R.G.; Inman, M.E.; Hudson, J.L. Analysis of electrochemical noise for type 410 stainless steel in chloride solutions. In *Electrochemical Noise Measurement for Corrosion Applications: ASTM STP 1277*; Kearns, J.R., Scully, J.R., Roberge, P.R., Eds.; American Society for Testing and Materials: West Conshohocken, PA, USA, 1996; pp. 101–103.
60. Okeniyi, J.O.; Popoola, A.P.I.; Loto, C.A. Corrosion test-data modeling for $C_{10}H_{18}N_2Na_2O_{10}$ performance on steel-rebar in NaCl-immersed concrete. In *CORROSION 2015*; NACE International: Houston, TX, USA, 2015.
61. Bouhrira, K.; Chetouani, A.; Zerouali, D.; Hammouti, B.; Yahyi, A.; Et-Touhami, A.; Yahyaoui, R.; Touzani, R. Theoretical investigation of inhibition of the corrosion of A106 steel in NaCl solution by di-*n*-butyl bis (thiophene-2-carboxylato-O,O′) tin (IV). *Res. Chem. Intermed.* **2014**, *40*, 569–586. [CrossRef]
62. Asegbeloyin, J.; Ejikeme, P.; Olasunkanmi, L.; Adekunle, A.; Ebenso, E. A novel Schiff base of 3-acetyl-4-hydroxy-6-methyl-(2*H*)pyran-2-one and 2,2′-(ethylenedioxy)diethylamine as potential corrosion inhibitor for mild steel in acidic medium. *Materials* **2015**, *8*, 2918–2934. [CrossRef]
63. Peme, T.; Olasunkanmi, L.; Bahadur, I.; Adekunle, A.; Kabanda, M.; Ebenso, E. Adsorption and corrosion inhibition studies of some selected dyes as corrosion inhibitors for mild steel in acidic medium: Gravimetric, electrochemical, quantum chemical studies and synergistic effect with Iodide ions. *Molecules* **2015**, *20*, 16004–16029. [CrossRef] [PubMed]
64. Afia, L.; Salghi, R.; Zarrouk, A.; Zarrok, H.; Bazzi, E.H.; Hammouti, B.; Zougagh, M. Comparative study of corrosion inhibition on mild steel in HCl medium by three green compounds: Arganiaspinosa press cake, kernels and hulls extracts. *Trans. Indian Inst. Met.* **2013**, *66*, 43–49. [CrossRef]
65. Foo, K.Y.; Hameed, B.H. Insights into the modeling of adsorption isotherm systems. *Chem. Eng. J.* **2010**, *156*, 2–10. [CrossRef]
66. Mehrizad, A.; Aghaie, M.; Gharbani, P.; Dastmalchi, S.; Monajjemi, M.; Zare, K. Comparison of 4-chloro-2-nitrophenol adsorption on single-walled and multi-walled carbon nanotubes. *Iran. J. Environ. Health Sci. Eng.* **2012**, *9*, 1–6. [CrossRef] [PubMed]
67. Bungey, J.H.; Millard, S.G.; Grantham, M.G. *Testing of Concrete in Structures*, 4th ed.; Taylor & Francis: New York, NY, USA, 2006.
68. Broomfield, J.P. *Corrosion of Steel in Concrete: Understanding, Investigation and Repair*; Taylor & Francis e-Library: New York, NY, USA, 2003.
69. McCarter, W.J.; Vennesland, Ø. Sensor systems for use in reinforced concrete structures. *Constr. Build. Mater.* **2004**, *18*, 351–358. [CrossRef]
70. Coffey, R.; Dorai-Raj, S.; O'Flaherty, V.; Cormican, M.; Cummins, E. Modeling of pathogen indicator organisms in a small-scale agricultural catchment using SWAT. *Hum. Ecol. Risk Assess. Int. J.* **2013**, *19*, 232–253. [CrossRef]
71. Okeniyi, J.O.; Ambrose, I.J.; Oladele, I.O.; Loto, C.A.; Popoola, P.A.I. Electrochemical performance of sodium dichromate partial replacement models by triethanolamine admixtures on steel-rebar corrosion in concretes. *Int. J. Electrochem. Sci.* **2013**, *8*, 10758–10771.
72. Okeniyi, J.O.; Ogunlana, O.O.; Ogunlana, O.E.; Owoeye, T.F.; Okeniyi, E.T. Biochemical characterisation of the leaf of *Morinda lucida*: Prospects for environmentally-friendly steel-rebar corrosion-protection in aggressive medium. In *TMS2015 Supplemental Proceedings*; John Wiley & Sons, Inc.: Hoboken, NJ, USA, 2015; pp. 635–644. [CrossRef]
73. Al-Amiery, A.; Al-Majedy, Y.; Kadhum, A.; Mohamad, A. New coumarin derivative as an eco-friendly inhibitor of corrosion of mild steel in acid medium. *Molecules* **2015**, *20*, 366–383. [CrossRef] [PubMed]
74. Kadhum, A.; Mohamad, A.; Hammed, L.; Al-Amiery, A.; San, N.; Musa, A. Inhibition of mild steel corrosion in hydrochloric acid solution by new coumarin. *Materials* **2014**, *7*, 4335–4348. [CrossRef]
75. Al-Amiery, A.; Kadhum, A.; Kadihum, A.; Mohamad, A.; How, C.; Junaedi, S. Inhibition of mild steel corrosion in sulfuric acid solution by new Schiff base. *Materials* **2014**, *7*, 787–804. [CrossRef]
76. Morad, M.S. Corrosion inhibition of mild steel in sulfamic acid solution by S-containing amino acids. *J. Appl. Electrochem.* **2008**, *38*, 1509–1518. [CrossRef]